

Spectroscopic Evidence for a Gold-Coloured Metallic Water Solution

Philip E. Mason,^{1†} H. Christian Schewe,^{1,2†} Tillmann Buttersack,^{1,2,3†} Vojtech Kostal,¹ Marco Vitek,¹ Ryan S. McMullen,³ Hebatallah Ali,^{2,4} Florian Trinter,^{2,5,6} Chin Lee,^{2,7,8} Daniel M. Neumark^{7,8}, Stephan Thürmer,⁹ Robert Seidel,^{10,11} Bernd Winter,² Stephen E. Bradforth,³ and Pavel Jungwirth^{1*}

¹*Institute of Organic Chemistry and Biochemistry, Czech Academy of Sciences, Flemingovo nam. 2, 16610 Prague 6, Czech Republic, ²Molecular Physics, Fritz-Haber-Institut der Max-Planck-Gesellschaft, Faradayweg 4-6, D-14195 Berlin, Germany,*

³*Department of Chemistry, University of Southern California, Los Angeles, CA 90089-0482, USA, ⁴Department of Physics, Women Faculty for Art, Science and Education, Ain Shams University, Heliopolis, 11757, Cairo, Egypt, ⁵Photon Science, Deutsches Elektronen-Synchrotron (DESY), Notkestr. 85, D-22607 Hamburg, Germany, ⁶Institut für Kernphysik, Goethe-Universität Frankfurt, Max-von-Laue-Str. 1, D-60438 Frankfurt am Main, Germany, ⁷Department of Chemistry, University of California, Berkeley, CA 94720, USA, ⁸Chemical Sciences Division, Lawrence Berkeley National Laboratory, Berkeley, CA 94720, USA, ⁹Department of Chemistry, Graduate School of Science, Kyoto University, Kitashirakawa-Oiwakecho, Sakyo-Ku, Kyoto 606-8502, Japan, ¹⁰Helmholtz-Zentrum Berlin für Materialien und Energie, Albert-Einstein-Straße 15, D-12489 Berlin, Germany, ¹¹Humboldt-Universität zu Berlin, Department of Chemistry, Brook-Taylor-Str. 2, D-12489 Berlin, Germany*

*Correspondence to: pavel.jungwirth@uochb.cas.cz

†All three authors contributed equally.

Attempts to convert pure water from an insulator into a metal by pressurizing the system remain in the realm of science fiction, since the estimated required pressure¹ of 48 Mbar is an order of magnitude higher than what is feasible in the laboratory nowadays and may only exist in cores of large planets or stars²⁻⁴. Indeed, recent estimates show that at experimentally accessible pressures one can reach at best superionic water with high protonic conductivity⁵, but not metallic water with conductive electrons¹. Here, we show that a metallic water solution can be prepared by massive doping by electrons liberated from alkali metals. Analogous metallic solutions of liquid ammonia, which may serve in many respects as a proxy to water, have been characterized previously⁶⁻⁹. However, it is a textbook knowledge that dissolution of alkali metals in water leads to an explosive chemical reaction^{10,11}, thus aqueous solutions with only low (sub-metallic) electron concentrations have been prepared so far¹²⁻¹⁴. We have now found a way around the explosive chemistry by adsorbing water vapour at a pressure of about 10^{-4} mbar onto a train of liquid sodium-potassium alloy drops ejected from a nozzle into a vacuum chamber. This leads to a formation of a transient gold-coloured layer of water doped with $\sim 5 \times 10^{21}$ electrons/cm³, the metallic character of which is demonstrated by a combination of optical reflection and synchrotron x-ray photoelectron spectroscopies.

Water adsorption on sodium-potassium alloy drops

The current experiment is realized with a sodium-potassium (NaK) alloy, which is liquid at room temperature^{15,16}, dripping at a rate of about one drop per 10 s from a micro-nozzle into a vacuum chamber with a background water vapour pressure tunable up to a fraction of a millibar. With no water vapour in the vacuum chamber the NaK drops have no distinct colour, but only a silver metallic sheen (for a representative snapshot see the top left panel of Figure 1). The lack of visible colour is due to the fact

that unlike transition metals, alkali metals have no *d* or *f* electrons subject to optical excitations. Also, except for cesium, their plasmon frequency is far in the UV region.^{9,16,17}.

When water vapour pressure in the vacuum chamber is increased to $\sim 10^{-4}$ mbar, a sufficient amount of water adsorbs at the surface of the newly formed NaK drops such that their surface layer turns almost immediately gold in colour (Figure 1). The golden colour persists for up to ~ 5 s, after which, as water keeps adsorbing further, the colour gradually turns into bronze for another 2–3 s (Figure 1). Eventually, the drop loses its metallic sheen turning purple-blue and finally white - the latter due to formation of an alkali hydroxide layer (Figure 1) as a product of the reaction of electrons with water. The whole process lasts for about 10 s, within which the drop grows and reaches its final size of ~ 5 mm in diameter, eventually falling off from the capillary end due to gravitational force, with a new drop starting to evolve immediately afterwards. The transient formation of a gold-coloured drop is completely reproducible for a “train” of hundreds of drops, provided the water vapour pressure is kept in a relatively narrow range close to the optimal values of about 10^{-4} mbar.

At this pressure, we can estimate using the Langmuir model¹⁸ that the aqueous layer at the NaK drop grows at a rate of ~ 80 monolayers per second, i.e., it thickens by about 24 nm/s. This estimate assumes that an impinging water vapour molecule has a diameter of 0.3 nm and a surface sticking probability of unity (for a schematic picture see Figure 2). The current situation differs from previous experiments where a single or a very small number of water monolayers were grown on potassium (or by co-adsorption of water with alkali metal on an inert metal substrate) at significantly lower water vapour pressures of $\sim 10^{-6}$ mbar and at cryogenic substrate temperatures around 100 K^{19,20}. In those early studies, electrons liberated from the alkali metal into the water monolayer transiently formed upon annealing individual partially hydrated electrons, which then

reacted toward hydrogen and hydroxide^{19,20}.

The key point regarding water adsorption on the alkali metal in the current experiment (Figure 2) is that dissolution of electrons and alkali cations in water^{11,21} is a much faster process than the growth of the aqueous layer^{18,22}. What is being built up on the NaK drop is thus not pure water but rather an aqueous layer doped with electrons, as well as with alkali cations. Unlike pure water, multiple layers of such an aqueous solution can apparently be grown under the current experimental conditions. This is a dynamical process, within which the formed layer is unlikely to be fully homogeneous. While in future studies it would be challenging to investigate in detail the spectroscopic signatures of all the stages of the evolution of the aqueous surface of the NaK drop, including the metal-to-electrolyte transition^{6,9} and the accompanying chemical transformations; here, we focus on the early phase characterized by the golden colour of the surface of the drop.

Optical and photoelectron spectra

For the gold-coloured drops, we recorded optical reflectance and x-ray photoelectron (PE) spectra and compared them to those of pure NaK drops (Figure 3). For optical spectroscopy, we imaged the reflected light from a $\sim 1 \text{ mm}^2$ spot at the NaK drop surface and recorded reflection spectra using a commercial UV/VIS spectrometer (for details including calibration see Methods and SI). As mentioned above, pure NaK is colourless and the corresponding reflection-mode optical spectrum thus reflects the distribution of spectral intensity of the incandescent lightbulb used for illuminating the sample (black line in Figure 3a). With water vapour in the chamber the formation of the gold-coloured aqueous layer on the NaK drop is manifested in the spectrum by occurrence of a prominent broad absorption feature at a wavelength range of 400 – 600 nm, see Figure 3a,b. A fully quantitative Lorentzian fit to these measured data in energy units is presented in Figure 4a yielding a peak at 2.74 eV (corresponding to 452 nm) with a full width at half maximum (FWHM) of 0.59 eV.

Analogously to metallic alkali metal – liquid ammonia solutions⁹, we can connect the observed metallic golden colour to the plasmon frequency pertinent to the free electron gas²³ of the metallic water solution. However, unlike the bulk metallic solutions of alkali metals in liquid NH₃, which reflect light below the plasmon frequency and are transparent to light at higher frequencies⁹, here we additionally observe absorption of light around the plasmon frequency. Note that in bulk systems light as transverse electromagnetic radiation is from symmetry reasons unable to excite plasmons, which are longitudinal waves²³. The key point here is that metallic water solution is formed in the current experiments as a thin layer in which optical excitation of a plasmon becomes feasible at around the plasmon frequency²⁴ (see SI for further details).

An interesting feature in the spectrum is that the reflectivity at frequencies above the plasmon absorption band increases again (Figure 3a,b). The metallic water solution, like any other simple metal, becomes transparent for radiation of frequencies higher than the plasmon frequency and hence its reflectivity would not be expected to recover. However, in the current case of a thin metallic water layer, high-frequency radiation which is transmitted through it is in fact reflected from the underlying pure NaK, which has its plasmon frequency only at around 275 nm (corresponding to 4.5 eV).

Optical measurements were complemented in an analogous setup by synchrotron radiation x-ray PE spectroscopy. PE spectra at photon energy of 330 eV were acquired in the so-called fixed-mode that allows simultaneous recording of a 9 eV wide spectral window with a sampling rate of ~0.6 Hz, i.e., every 1.6 s a spectrum is recorded (for more details see Methods and SI). The spectrum collected from NaK drops ejected into the vacuum chamber in the absence of water vapour (black line in Figure 3c) is almost identical to that obtained from a pure NaK microjet previously⁹ (see also SI). The main PE spectral features of pure NaK are a ~2 eV wide conduction band, with a sharp Fermi edge defining here zero binding energy, and a Lorentzian-shaped plasmon peaking at

around 4.5 eV (Figure 3c and Ref. 9).

Due to water vapour adsorption on the NaK drops, the PE spectrum (golden line in Figure 3c) changes in three distinct ways. First, an additional peak appears at 2.7 eV with FWHM of \sim 0.6 eV on a rather shallow spectral background (Figures 3c and 4b), which quantitatively matches the value of the metallic water plasmon energy observed in the optical spectrum (Figure 3a,b). Second, there appears a new feature near the Fermi edge²³, which we interpret as a narrow (\sim 1.1 eV) conduction band of the metallic water solution on top of a wider (\sim 2 eV) conduction band of pure NaK (Figure 3c). It is important to reiterate here that the drop is a dynamic system that grows and spins during the measurement. Typically, only part of the region on the drop's surface that is probed by x-rays consists of a metallic water layer, with the remainder being pure NaK alloy. Therefore, the recorded PE spectrum is a sum of contributions from the metallic water solution and pure NaK (Figure 3c). Third, a strong signal rises at higher binding energies with an onset around 5.3 eV from the Fermi level. The limited energy window within the fixed-mode data acquisition did not allow for simultaneous measurement of PE peaks of all the species present (i.e., excess electrons, water, alkali cations, and hydroxide anions), nevertheless we clearly see water signal in the PE spectra acquired in the sweep-mode integrated over the drop lifetime (see SI for more details). Also, the observed onset of the spectra in Figure 3c occurs in the spectral region where signal from hydroxide, both aqueous²⁵ and solid²⁶, should start to appear. As the drop matures, we observe a shift of about 0.3 eV of this onset toward higher binding energies (see SI). An analogous shift was noticed previously for aqueous hydroxide upon increasing its concentration²⁵. This indicates that before a visible crust of solid alkali hydroxide is formed at the later stages of the drop's development, hydroxide is dissolved in the thin layer of metallic water.

The decomposition of the PE spectrum into contributions from the metallic water solution and NaK, with conduction bands and plasmons fitted using the free electron gas

model, assuming a Lorentzian shape of the plasmon peaks, is presented in Figure 4b (see SI for more details). Given the simplicity of the model, where the only parameter is the density of free electrons, it is remarkable how well it fits the experimental data. The value of the obtained free electron density is about $5 \times 10^{21} \text{ cm}^{-3}$, which corresponds to a concentration of $\sim 18 \text{ MPM}$. This estimated value for the metallic aqueous solutions of sodium and potassium is likely to be close to the saturation limit, being consistent with solubilities of these alkali metals in liquid ammonia reaching $\sim 20 \text{ MPM}$ (with the electrolyte-to-metal transition occurring at around $1 - 5 \text{ MPM}$)⁶. Also note that the free electron density of the metallic water solution is about three times lower than that of pure NaK⁹, which is in line with the UV-to-visible shift of the plasmon peak and a conduction band of about half the width when comparing the former with the latter system (Figure 4b).

Discussion and Conclusions

We have shown here that exposing NaK drops to vapor pressure of $\sim 10^{-4} \text{ mbar}$ leads to an almost immediate formation of a gold-coloured layer of a metallic water solution. The gold colour cannot be due to interference effects since it appears already when the layer is more than an order of magnitude thinner than the corresponding wavelength region of 400 - 600 nm. Moreover, we do not observe any red-to-blue colour shift that would be characteristic to interference from a layer growing to a thickness approaching wavelengths of the blue edge of the visible spectrum. The gold colour with its characteristic sheen is instead a signature of a metallic character of the surface layer.

The relatively long lifetime of several seconds of the metallic water layer is partly due to the presence of the underlying alkali metal providing excess electrons in a quasi-steady state manner; this is similar to our earlier experiments, where putting sodium-potassium alloy next to a water drop led to transient formation of a blue electrolyte layer of hydrated electrons at elevated temperature¹³. In addition, it is plausible that hydrated

electrons become less reactive and thus longer-lived upon delocalization in the metallic regime. This effect could be rationalized by the fact that for localized hydrated electrons there is a better chance to react with adjacent water molecules than for delocalized electrons in the conduction band of the metallic solution. The lifetime of dilute localized hydrated electrons is sub-millisecond²⁷, while in the current experiments the metallic water layer persists for seconds. Still, chemistry starts early on as evidenced by the presence of a signal from hydroxide in the PE spectra. The metallic water solution should thus be understood as a dynamically evolving system of a high concentration of excess electrons forming a conduction band and alkali metal cations. Moreover, as chemistry proceeds during the drop development, hydroxide anions and hydrogen form, leading to an increasingly concentrated aqueous hydroxide solution as well as to solid hydroxide. Consistent with earlier observations of a blue colour of electrons in strongly alkaline amorphous ices^{28,29}, this effect together with further water adsorption is likely causing the change of colour to purple/blue as the drop matures (Figure 1).

In conclusion, by adsorbing water vapour on a NaK drop rather than dissolving alkali metals in liquid water, we managed to keep the vigorous (even explosive) chemical reactivity temporarily at bay in a manner sufficient for spectroscopic characterization of the formed gold-coloured layer of a metallic water solution. In this way, we were able to bypass the need for employing unrealistically high pressures¹ for metallization of water.

Methods

Liquid sodium-potassium alloy (NaK) was made by mixing solid sodium and solid potassium (1:1 mol-ratio, 99.8% Sigma-Aldrich). Details are provided in Ref. ¹¹ and in the SI. For acquiring both optical and PE spectra we used our modified microjet setup described in Ref. ³⁰ to produce drops (as well as micro-sized jets) of NaK and we added a water supply line to transfer water vapor at pressures varying from 10^{-5} to 2×10^{-4} mbar into our vacuum chamber. By reducing the argon pressure above the NaK reservoir, the

continuous NaK jet turns into a periodic drop train, which was essential for tracking formation of the metallic water solution on the drop surface.

Optical reflection measurements

The optical reflection measurements, described in more detail in the SI and in a Supplementary Video, were conducted at IOCB Prague. In a typical experiment, we created NaK drops at a rate of one drop every \sim 10 s with spectra recorded with the AvaSpecULS 2048 spectrometer every 0.1–0.3 s. We synchronized the saving of the time stamp of each spectrum by recording a video where the image of the drop taken with a CCD camera is shown together with the current time to directly relate the sampled spectra to the size and colour of the NaK drop at a given moment in time.

First, we took as reference the reflection spectra of pure NaK drops, the surface of which is highly reflective in the infrared and visible parts of the electromagnetic spectrum (up to its plasmon frequency of \sim 4.5 eV). Next, water vapor was transferred into the vacuum chamber via a tube from a water reservoir with the amount of vapour being controlled using a needle valve. We found the NaK drop to turn golden for several seconds within a pressure range of 6×10^{-5} - 2×10^{-4} mbar with an optimal performance at $\sim 10^{-4}$ mbar. The spectra taken at this water vapour pressure were normalized using the reflection spectra of pure NaK.

Synchrotron-based photoelectron spectroscopy measurements

X-ray PE spectroscopy measurements were performed using the SOL³PES setup²⁷ connected to the U49-2_PGM-1 beamline²⁸ of the synchrotron radiation facility BESSY II in Berlin (see SI for more details). Similarly to the optical measurements, experiments were performed under vacuum conditions (10^{-5} mbar) with or without the presence of water vapour at a pressure of $\sim 10^{-4}$ mbar, with a NaK drop rate of 0.1 Hz. Drops were

irradiated on the upper part by horizontally polarized soft x-ray light. Water vapour was directed onto the same surface spot where the x-ray photons hit the NaK drop. The emitted photoelectrons were detected by a ScientaOmicron R4000 HiPP-2 hemispherical electron analyzer mounted in the same plane as the polarization axis. Valence PE spectra were measured at a photon energy of 330 eV using a pass energy of 100 eV. This large pass energy allowed us to detect within the fixed-mode setting of the electron analyzer a 9-eV wide kinetic energy window in one shot, which was enough to record the conduction band with its Fermi edge and the plasmon features, as well as the onset of the hydroxide peak.

A sampling rate of ~0.6 Hz (with a spectrum being recorded for 0.4 s followed by 1.2 s of a dead time due to saving the data) was chosen to guarantee a sufficient time resolution as well as a good enough signal-to-noise ratio. Details of this data acquisition mode and the corresponding data analysis and fitting procedures are described in the SI.

Data availability

The data sets generated during the current study are available as Supplementary Data or are available from the corresponding author upon reasonable request.

Code availability

Data-processing and fitting results can be generated using numerical methods described in Methods and Supplementary Information and developed computer codes that are available upon reasonable request.

References

- 1 Hermann, A., Ashcroft, N. W. & Hoffmann, R. High pressure ices. *Proceedings of the National Academy of Sciences of the United States of America* **109**, 745-750, doi:10.1073/pnas.1118694109 (2012).
- 2 Dubrovinsky, L., Dubrovinskaia, N., Prakapenka, V. B. & Abakumov, A. M. Implementation of micro-ball nanodiamond anvils for high-pressure studies above 6 Mbar. *Nature Communications* **3**, doi:10.1038/ncomms2160 (2012).
- 3 Cavazzoni, C., Chiarotti, G. L., Scandolo, S., Tosatti, E., Bernasconi, M. & Parrinello, M. Superionic and metallic states of water and ammonia at giant planet conditions. *Science* **283**, 44-46, doi:10.1126/science.283.5398.44 (1999).
- 4 Mattsson, T. R. & Desjarlais, M. P. Phase diagram and electrical conductivity of high energy-density water from density functional theory. *Physical Review Letters* **97**, doi:10.1103/PhysRevLett.97.017801 (2006).
- 5 Millot, M., Coppapi, F., Rygg, J. R., Barrios, A. C., Hamel, S., Swift, D. C. & Eggert, J. H. Nanosecond X-ray diffraction of shock-compressed superionic water ice. *Nature* **569**, 251-255, doi:10.1038/s41586-019-1114-6 (2019).
- 6 Zurek, E., Edwards, P. P. & Hoffmann, R. A Molecular Perspective on Lithium-Ammonia Solutions. *Angewandte Chemie-International Edition* **48**, 8198-8232, doi:10.1002/anie.200900373 (2009).
- 7 Thompson, J. C. *Electrons in Liquid Ammonia*. (Clarendon Press, 1976).
- 8 Lodge, M., Cullen, P., Rees, N. H., Spencer, N., Maeda, K., Harmer, J. R., Jones, M. O. & Edwards, P. P. Multielement NMR Studies of the Liquid-Liquid Phase Separation and the Metal-to-Nonmetal Transition in Fluid Lithium- and Sodium-Ammonia Solutions. *Journal of Physical Chemistry B* **117**, 13322-13334, doi:10.1021/jp404023j (2013).
- 9 Buttersack, T., Mason, P. E., McMullen, R., Schewe, H. C., Martinek, T., Brezina, K., Crhan, M., Gomez, A., Hein, D., Wartner, G., Seidel, R., Ali, H., Thurmer, S., Marsalek, O., Winter, B., Bradforth, S. E. & Jungwirth, P. Photoelectron spectra of alkali metal-ammonia microjets: From blue electrolyte to bronze metal. *Science* **368**, 1086-1091, doi:10.1126/science.aaz7607 (2020).
- 10 Hutton, A. T. Dramatic Demonstration for a Large Audience - The Formations of Hydroxyl Ions in the Reaction of Sodium with Water *Journal of Chemical Education* **58**, 506-506 (1981).
- 11 Mason, P. E., Uhlig, F., Vanek, V., Buttersack, T., Bauerecker, S. & Jungwirth, P. Coulomb explosion during the early stages of the reaction of alkali metals with water. *Nature Chemistry* **7**, 250-254, doi:10.1038/nchem.2161 (2015).
- 12 Young, R. M. & Neumark, D. M. Dynamics of Solvated Electrons in Clusters. *Chemical Reviews* **112**, 5553-5577, doi:10.1021/cr300042h (2012).
- 13 Mason, P. E., Buttersack, T., Bauerecker, S. & Jungwirth, P. A Non-Exploding Alkali Metal Drop on Water: From Blue Solvated Electrons to Bursting Molten Hydroxide. *Angewandte Chemie-International Edition* **55**, 13019-13022, doi:10.1002/anie.201605986 (2016).
- 14 Suzuki, T. Ultrafast photoelectron spectroscopy of aqueous solutions. *Journal of Chemical Physics* **151**, doi:10.1063/1.5098402 (2019).
- 15 Alchagirov, B. B., Afaunova, L. K., Dyshekova, F. F., Kegadueva, Z. A., Mozgovoi, A. G., Arkhestov, R. K., Taova, T. M. & Khokonov, K. B. Surface Tension and Adsorption of Components in the Sodium–Potassium Alloy Systems: Effective Liquid Metal Coolants Promising in Nuclear and Space Power

Engineering. *Inorganic Materials: Applied Research* **2**, 461-467 (2011).

16 Addison, C. C. *The Chemistry of Liquid Alkali Metals*. (John Wiley & Sons, 1984).

17 Citrin, P. H. High-Resolution X-Ray Photoemission from Sodium Metal and its Hydroxide *Physical Review B* **8**, 5545-5556, doi:10.1103/PhysRevB.8.5545 (1973).

18 Lueth, H. *Surfaces and Interfaces of Solid Materials*. (Springer, 1997).

19 Kiskinova, M., Pirug, G. & Bonzel, H. P. Adsorption and Decomposition of H₂O on a K-Covered Pt(111) Surface. *Surface Science* **150**, 319-338, doi:10.1016/0039-6028(85)90649-1 (1985).

20 Blass, P. M., Zhou, X. L. & White, J. M. Coadsorption and Reaction of Water and Potassium on Ag(111). *Journal of Physical Chemistry* **94**, 3054-3062, doi:10.1021/j100370a058 (1990).

21 Nachtrieb, N. H. Self-Diffusion in Liquid Metals. *Advances in Physics* **16**, 309-+, doi:10.1080/00018736700101425 (1967).

22 Ketteler, G., Yamamoto, S., Bluhm, H., Andersson, K., Starr, D. E., Ogletree, D. F., Ogasawara, H., Nilsson, A. & Salmeron, M. The nature of water nucleation sites on TiO₂(110) surfaces revealed by ambient pressure X-ray photoelectron spectroscopy. *Journal of Physical Chemistry C* **111**, 8278-8282, doi:10.1021/jp068606i (2007).

23 Kittel, C. *Introduction to Solid State Physics*. (John Wiley & Sons, Inc., 2005).

24 Abeles, F., Borensztein, Y., Decrescenzi, M. & Lopezrios, T. Optical Evidence for Longitudinal-Waves in Very Thin Ag Layers. *Surface Science* **101**, 123-130, doi:10.1016/0039-6028(80)90603-2 (1980).

25 Winter, B., Faubel, M., Vacha, R. & Jungwirth, P. Behavior of hydroxide at the water/vapor interface. *Chemical Physics Letters* **474**, 241-247 (2009).

26 Bonzel, H. P., Pirug, G. & Winkler, A. Adsorption of H₂O on Potassium Films. *Surface Science* **175**, 287-312, doi:10.1016/0039-6028(86)90237-2 (1986).

27 Hart, E. J. & Boag, J. W. Absorption Spectrum of Hydrated Electron in Water and in Aqueous Solutions. *Journal of the American Chemical Society* **84**, 4090-4095 (1962).

28 Barzynski, H. & Schulte-Frohlinde, D. On the Nature of the Electron Traps in Alkaline Ice. *Zeitschrift Fur Naturforschung Section a-a Journal of Physical Sciences* **22**, 2131-2132 (1967).

29 Kevan, L. Slovated Electron Structure in Glassy Matrices. *Accounts of Chemical Research* **14**, 138-145, doi:10.1021/ar00065a002 (1981).

30 Buttersack, T., Mason, P. E., Jungwirth, P., Schewe, C., Winter, B., Seidel, R., McMullen, R. & Bradforth, S. E. Deeply Cooled and Temperature Controlled Microjets: Liquid Ammonia Solutions Released into Vacuum for Analysis by Photoelectron Spectroscopy. *Review of Scientific Instruments* **91**, 043101, doi:DOI: 10.1063/1.5141359 (2020).

Supplementary information is linked to the online version of the paper at www.nature.com/nature .

Acknowledgments

P.J. acknowledges support from the European Regional Development Fund (project ChemBioDrug no. CZ.02.1.01/0.0/0.0/16_019/0000729). D.M.N. and C.L. acknowledge support from the Director, Office of Basic Energy Science, Chemical Sciences Division of the U.S. Department of Energy under Contract No. DE-AC02-05CH11231 and the Alexander von Humboldt Foundation. S.E.B., T.B., and R.S.M. are supported by the US National Science Foundation (CHE-1665532). P.E.M. acknowledges support from the viewers of his YouTube popular science channel. C.T. acknowledge support from the Charles University in Prague and from the International Max Planck Research School in Dresden. S.T. acknowledges support from the JSPS KAKENHI Grant No. JP18K14178. RS acknowledges the German Research Foundation for an Emmy-Noether Young-Investigator stipend (DFG, project SE 2253/3-1). F.T. and B.W. acknowledge support by the MaxWater initiative of the Max-Planck-Gesellschaft. All authors thank the staff of the Helmholtz-Zentrum Berlin for their support during the beamtimes at BESSY II.

Author contribution

P.E.M., H.C.S., T.B., B.W., S.E.B., and P.J. designed the experiments, P.E.M., H.C.S., T.B., B.W., H.A., V.K., M.V., F.T., C.L., D.M.N., R.S., and P.J performed the experiments, and P.E.M., H.C.S., T.B., B.W., S.E.B., R.S.M., C.L., R.S., S.T., and P.J analyzed the obtained data. P.J. wrote the main paper, while H.C.S. and P.J. wrote the Supplementary Information, both with critical feedback from all the co-authors. P.E.M. produced the Supplementary Video.

Competing Interests statement

The authors declare that they have no competing financial interests.

Additional information

Supplementary information The online version contains supplementary material available at ...

Correspondence and requests for materials should be addressed to P.J. (e-mail: pavel.jungwirth@uochb.cas.cz).

Peer review information Peer reviewer reports are available.

Reprints and permissions information is available at <http://www.nature.com/reprints>

Figure captions:

Figure 1: A pure NaK drop in vacuum vs. time evolution of a NaK drop exposed to water vapour. A fresh drop of sodium-potassium alloy ejected from a quartz capillary into the vacuum chamber without the presence of water vapour (top left). This silver drop lacks any distinct colour. Next, we show eight snapshots recording the second-by-second time evolution of a sodium-potassium alloy drop ejected from a micro-nozzle into the vacuum chamber with a background water vapor pressure of $\sim 10^{-4}$ mbar. The snapshots demonstrate an early formation of a gold-coloured layer of a metallic water solution, which due to further water adsorption turns within several seconds into bronze and blue losing eventually its metallic sheen, with visible white patches of the formed alkali hydroxide. At the end of the ~ 10 s cycle, the drop reaches a final diameter of about 5 mm, after which it detaches from the capillary and a new drop starts forming.

Figure 2: A schematic picture demonstrating formation of a thin gold-coloured metallic water layer by water vapour adsorption on a NaK drop. The dynamical process is characterized by a much faster dissolution of electrons and alkali cations^{11,21} than is the growth of the aqueous layer^{18,22}, which ensures high concentration of electrons throughout the system. At the same time, chemistry is taking place, leading to formation of hydroxide and hydrogen.

Figure 3: Spectroscopic signatures of metallic water solution from optical and x-ray photoelectroin spectroscopies. a,b) Optical reflection spectra and c) photoelectron spectra of the gold-coloured layer of a metallic water solution (partially) covering the NaK drop and analogous spectra of a pure sodium-potassium alloy drop. a) The reflection spectrum of the colourless pure NaK drop reflects the spectral characteristics of the illuminating lamp, which when subtracted b) yields for this system a flat spectrum, while exemplifying a prominent plasmonic absorption of the metallic water

layer. c) A typical photoelectron spectrum of a metallic water solution compared to a pure sodium-potassium alloy. The emerging spectral features upon exposure to $\sim 10^{-4}$ mbar of water vapour encompass occurrence of a new plasmon peak and of a narrow conduction band next to the Fermi edge. At the same time, we observe signal from hydroxide as a product of the chemical reaction between alkali metals and water.

Figure 4: Fits to the experimental data employing a free electron gas model. a) A Lorentzian fit to the plasmonic absorption feature in the optical reflection spectrum yielding a broad peak at 2.74 eV. b) Fits to averaged photoelectron spectra of NaK drops exposed to $\sim 10^{-4}$ mbar of water vapour, namely to the plasmon peaks (by Lorentzian functions) and conduction bands of both NaK and a metallic water solution using the free electron gas model. Formation of the gold-coloured metallic water layer is accompanied with an appearance of a plasmon peak at ~ 2.7 eV and a 1.1 eV wide conduction band conduction with a sharp Fermi edge at 0 eV (on top of a broader conduction band of pure NaK).

Figure 1

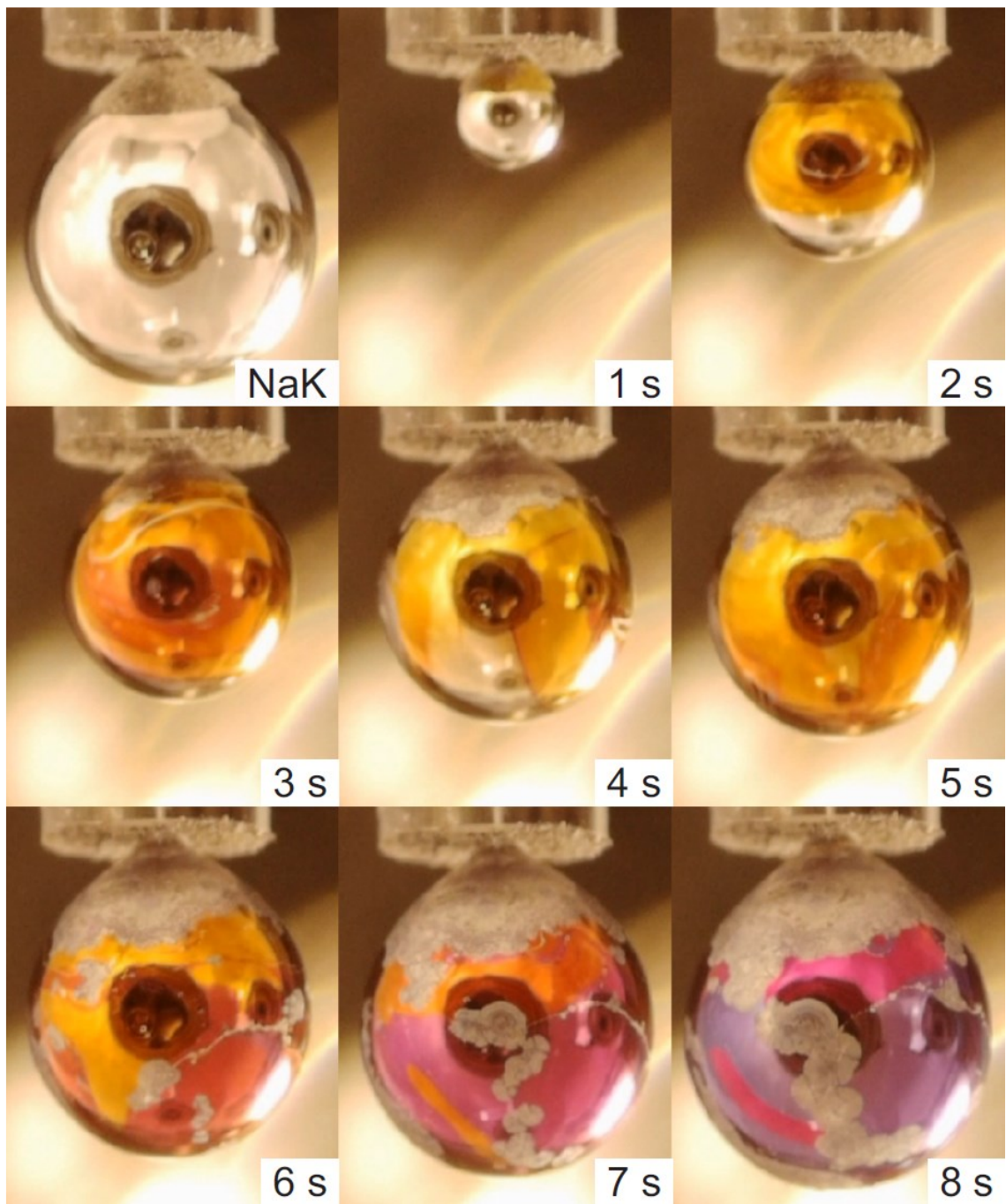


Figure 2

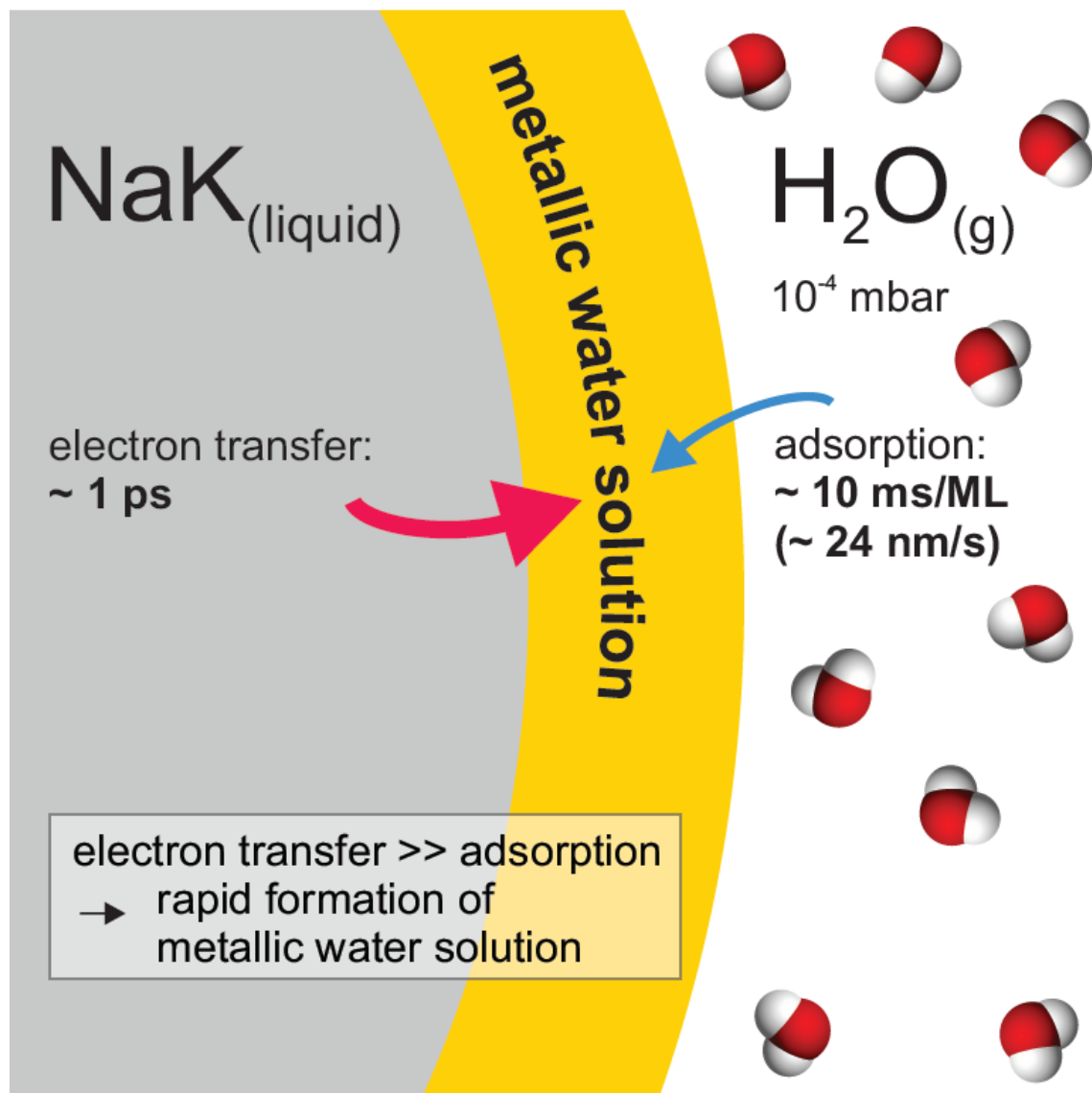


Figure 3

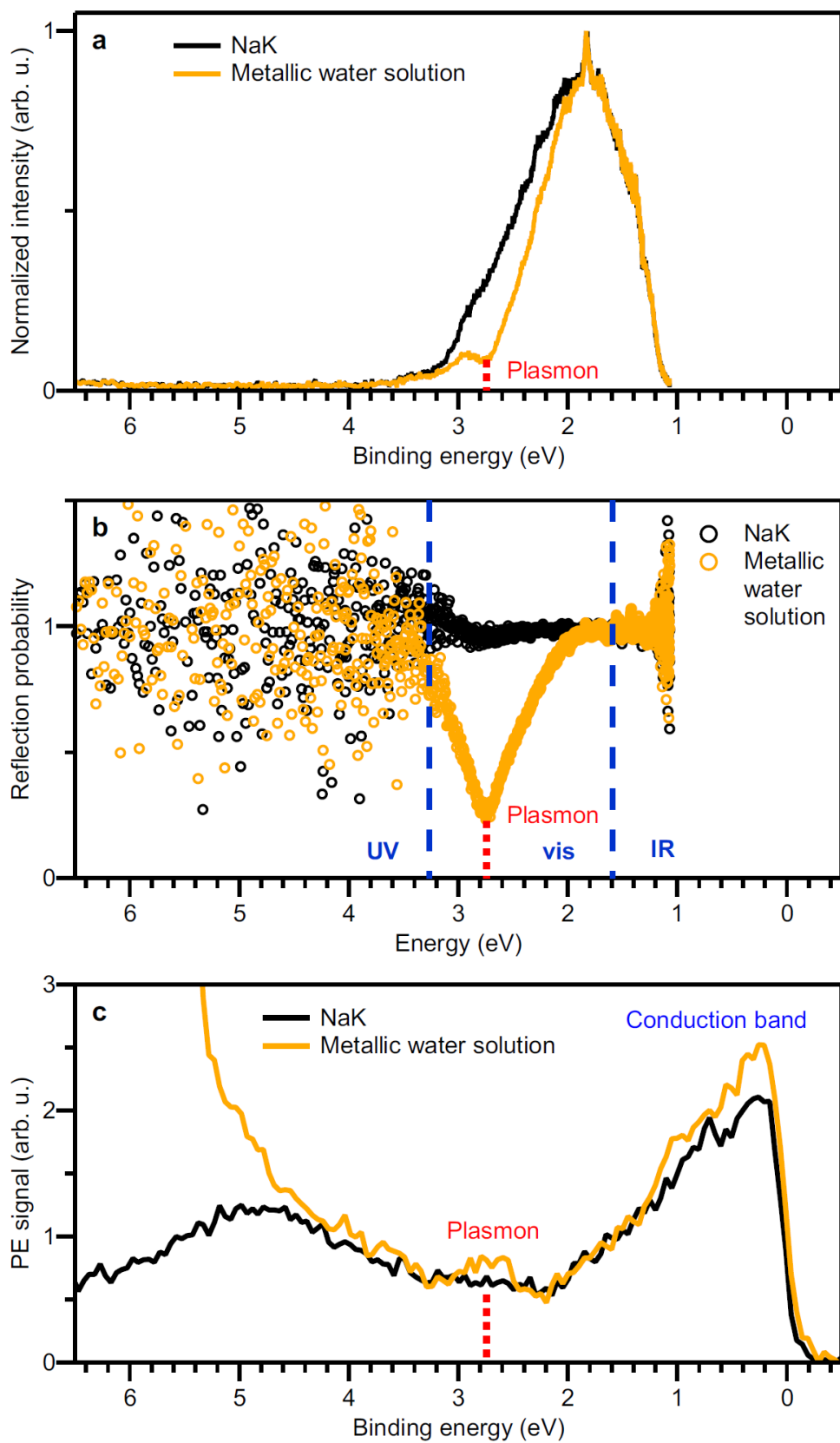


Figure 4

